Synthesis, structure, and catalytic activity of Keggin-type polyoxometalate coordinated Cu(I): {[Cu(py)$_2$]$_4$[SiW$_{12}$O$_{40}$]}, via hydrothermal decarboxylation

Rui Yang [a], Shu-Xia Liu [a], Qun Tang [a], Shu-Jun Li [a] & Da-Dong Liang [a]

[a] Key Laboratory of Polyoxometalates Science of Ministry of Education, College of Chemistry, Northeast Normal University, Changchun City, JiLin 130024, P.R. China
Version of record first published: 24 Feb 2012.

PLEASE SCROLL DOWN FOR ARTICLE

Taylor & Francis
Taylor & Francis Group

Synthesis, structure, and catalytic activity of Keggin-type polyoxometalate coordinated Cu(I): {[Cu(py)$_2$]$_4$[SiW$_{12}$O$_{40}$]}, *via* hydrothermal decarboxylation

RUI YANG, SHU-XIA LIU*, QUN TANG, SHU-JUN LI
and DA-DONG LIANG

Key Laboratory of Polyoxometalates Science of Ministry of Education, College of
Chemistry, Northeast Normal University, Changchun City,
JiLin 130024, P.R. China

A Keggin-type polyoxometalate [SiW$_{12}$O$_{40}$]$^{4-}$ supported transition metal complex, {[Cu(py)$_2$]$_4$[SiW$_{12}$O$_{40}$]} (py = pyridine), has been synthesized by hydrothermal decarboxylation and characterized by elemental analyses, IR spectra, thermal stability analyses, and single-crystal X-ray diffraction. The compound is a 1-D chain containing an inorganic–organic backbone with alternating [SiW$_{12}$O$_{40}$]$^{4-}$ clusters and [Cu(py)$_2$]$^+$ along the *c*-axis, and with both three- and four-coordinate copper. The luminescence properties indicated that the emission peak is emission of pyridine, assigned to the Cu(I) to pyridine charge transfer. This air-stable Cu(I) complex can efficiently catalyze the *O*-arylation of both phenols and aryl halides.

Keywords: Cu(I) compound; Polyoxometalates; Hydrothermal; Decarboxylation

1. Introduction

Polyoxometalates (POMs) have discrete structures of definite sizes and shapes, such as the Keggin, Dawson, Lindqvist, and Waugh [1]. As a rich and diverse class of inorganic cluster systems, POM ions are characterized by fascinating structural, electrochemical, catalytic, magnetic, medicinal, and photophysical properties [2]. POMs with Keggin structure continue to have an important place at the forefront of the POM field as a consequence of their unusual electronic versatility and structural diversity. A series of compounds made of Keggin POMs associated with transition metal coordination complex cations have been described [3–5]. Transition metal complexes having only three bonds or low coordination numbers are interesting because orbital energies, spin states, and reaction pathways can be different from those in traditional complexes [6]. Coordination number three for the late elements of the first transition series, notably those of Cu(I) with d^{10} electron configuration, is well-documented [7–9]. Copper ions play important roles in biology [10] and catalysis [11], and great effort has been

---

*Corresponding author. Email: liusx@nenu.edu.cn

expended to uncover mechanistic information and, in particular, to identify possible copper–oxygen intermediates [12].

Here a Keggin unit supported transition metal Cu(I) complex $\{[Cu(py)_2]_4[SiW_{12}O_{40}]\}$ (py = pyridine) has been obtained by hydrothermal decarboxylation reaction. The backbone of **1** is a 1-D linear chain comprising alternating $[SiW_{12}O_{40}]^{4-}$ clusters and Cu(I) ions along the *c*-axis. The luminescence and catalytic activities of this active and air-stable Cu(I) complex are described.

2. Experimental

2.1. *Materials and measurement*

All solvents and reagents are purchased from commercial sources. Elemental analyses are performed on a Perkin-Elmer 2400 CHN elemental analyzer. Infrared (IR) spectrum is recorded from 400 to 4000 cm^{-1} on an Alpha Centaurt FT/IR spectrophotometer using KBr pellet. Powder X-ray diffraction measurements are performed on a Rigaku D/MAX-3 instrument with Cu-Kα radiation in the angular range $2\theta = 3$–$60°$ at 293 K. Thermal stability analysis is performed on a Perkin-Elmer TGA7 instrument in flowing N_2 with a heating rate of $10°C\,min^{-1}$. Photoluminescence spectra are measured using an FLSP 920 Edinburgh instrument (Eng) with 450 W Xenon lamp monochromated by double grating.

2.2. *Synthesis of 1*

A mixture of $CuCl_2$ (0.268 g, 0.2×10^{-3} mol), isonicotinic acid (0.158 g, 0.2×10^{-3} mol), $H_4SiW_{12}O_{40} \cdot nH_2O$ (0.2 g), and H_2O (10 mL) is stirred for 30 min at room temperature, and the solution is adjusted to pH = 5.0–6.0 with triethylamine. Then the mixture is transferred and sealed in a 20 mL Teflon-lined stainless steel container. After being heated to 180°C under autogenous pressure for 5 days, the bomb is cooled to 100°C at the rate of $5°C\,h^{-1}$ and maintained for 10 h. After that the bomb is cooled to room temperature naturally and crystals of **1** are obtained. Compound **1** is collected as colorless leaf-shaped crystals with a yield of 45% (based on W). Elemental analysis for $C_{40}H_{40}Cu_4N_8O_{42}SiW_{12}$ (%): H, 1.05 (Calcd 1.06); C, 12.64 (12.67); N, 2.99 (2.95); Si, 0.71 (0.74); Cu, 6.69 (6.71); W, 58.19 (58.16).

2.3. *X-ray crystallography*

Crystal data for **1** are collected on a Rigaku R-AXIS RAPID IP diffractometer (graphite monochromated Mo-Kα radiation: $\lambda = 0.71073$ Å) at 298 K. The linear absorption coefficients, scattering factors for the atoms, and anomalous dispersion corrections are taken from International Tables for X-ray Crystallography [13]. The structure of **1** is solved by the direct method and refined by full-matrix least-squares on F^2 using the SHELXTL crystallographic software package [14]. All non-hydrogen atoms are refined anisotropically. Hydrogen atoms for py are fixed in ideal positions. The crystal data and structure refinement results are summarized in table 1.

Table 1. Crystal data and structural refinement for **1**.

Empirical formula	$C_{40}H_{40}Cu_4N_8O_{42}SiW_{12}$
Formula weight	3793.17
Crystal system	Triclinic
Space group	$P\bar{1}$
Unit cell dimensions (Å, °)	
a	12.123(5)
b	13.302(5)
c	13.366(5)
α	108.049(5)
β	115.446(5)
γ	103.088(5)
Volume (Å^3), Z	1680.4(11), 1
Calculated density (g cm^{-3})	3.748
Absorption coefficient (mm^{-1})	21.795
$F(000)$	1690
θ range for data collection (°)	3.16–29.27
Total data collected	12,635
Unique data	9184
R_{int}	0.0455
Goodness-of-fit on F^2	0.930
$R_1 [I > 2\sigma(I)]$[a]	0.0491
wR_2 (all data)[b]	0.0996

[a]$R_1 = \sum||F_o| - |F_c||/\sum|F_o|$; [b]$wR_2 = \{\sum[w(F_o^2 - F_c^2)^2]/\sum[w(F_o^2)^2]\}^{1/2}$.
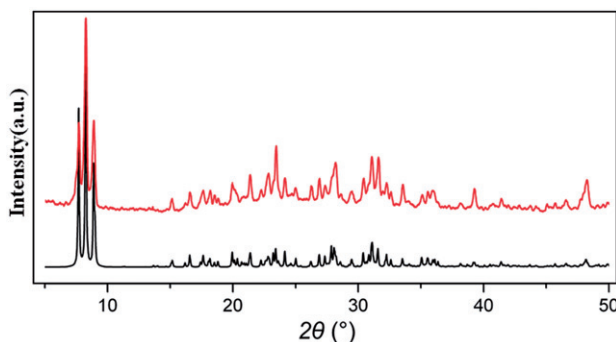
Figure 1. The XRPD patterns of **1**: simulated (bottom) and experimental (top).

The experimental and simulated X-ray powder diffraction patterns (XRPD) are shown in figure 1. The main diffraction peaks on experimental and simulated patterns match well in position, indicating its phase purity.

3. Results and discussion

3.1. *Synthesis*

Mixture of $CuCl_2$, isonicotinic acid, and $H_4SiW_{12}O_{40} \cdot nH_2O$ in water under hydro-thermal conditions gave crystals of **1** for X-ray diffraction. In the reaction pH,
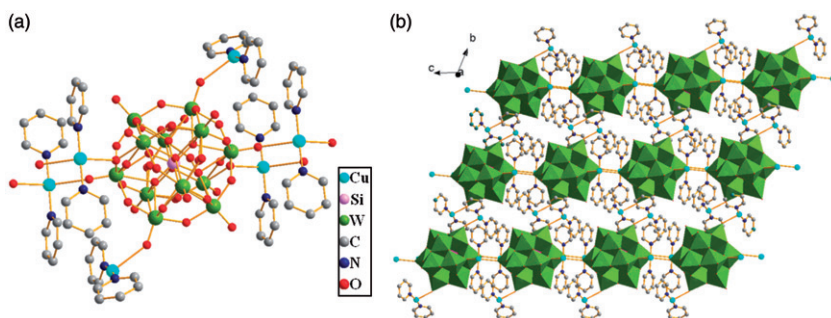
Figure 2.   (a) The coordination environment of Cu(I) in **1**; (b) polyhedral representation of the 1-D chain running along the *c*-axis of **1**.

temperature and reaction time are important. Compound **1** can be obtained in pH range 5.0–6.0. All Cu's in the resultant compound are reduced to univalent. We hypothesize that reduction of Cu(II) may be due to triethylamine. This process is usual under hydrothermal conditions. Similar reduction of Cu(II) to Cu(I) is observed in POMs bridged by copper complexes [15–17]. Removal of a carboxyl group from a compound, with hydrogen replacing it, can be performed by catalysis with Cu(I) [18, 19]. The decarboxylation reaction of the isonicotinic acid to pyridine is interpreted as the following equation. The space between the copper ions increases, because steric hindrance is reduced by decarboxylation. Thus, having available large number of exposed coppers will enhance catalytic activity, compared with similar complexes [20, 21].
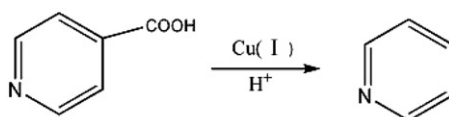
3.2. *Structure description*

Experimental details and single-crystal X-ray diffraction analysis data reveal that **1** consists of one $[SiW_{12}O_{40}]^{4-}$ and four $[Cu(py)_2]^+$ (figure 2a). The backbone of **1** is a 1-D linear chain comprising alternating $[SiW_{12}O_{40}]^{4-}$ clusters and Cu(I) along the *c*-axis (figure 2b). The heteropolyanion $[SiW_{12}O_{40}]^{4-}$ possesses the classical α-Keggin-type structure. Each Si(IV) is tetrahedrally coordinated and surrounded by four oxygen atoms (the O_{11}/O'_{11}, O_{20}/O'_{20} with disorder) with Si–O bonds ranging from 1.592 to 1.663 Å (mean 1.628 Å). All tungsten atoms have {WO_6} octahedral environments. The W–O bond distances are divided into three groups: W–Oa (center oxygen), 2.327–2.453 Å; W–Ob/c (bridging oxygen), 1.778–2.063 Å; W–Od (terminal oxygen), 1.647–1.715 Å. Each α-$SiW_{12}O_{40}$ cluster as a four-tooth ligand covalently bonds to four Cu(I)(py)$_2$ complexes through O6 and O19 of W_4O_{22} (W2, W6). The bond lengths around the four Cu(I) ions are 2.611 Å (Cu1–O19), 2.559 Å (Cu2–O6), 1.906–1.916 Å
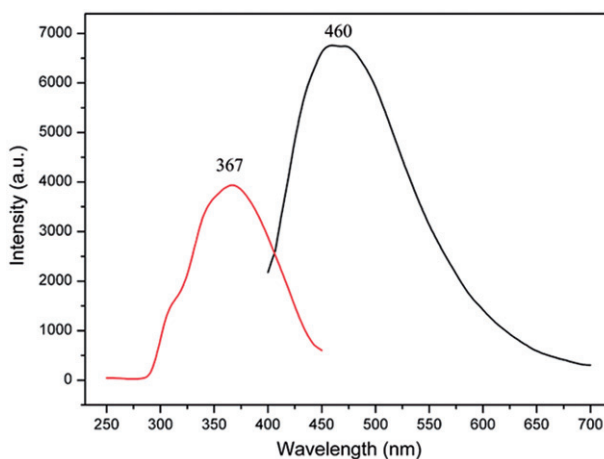
Figure 3.   The excitation (left) and emission (right) spectra of **1**.

(Cu1–N), 1.888–1.913 Å (Cu2–N), while the N–Cu–N angles are 168.26–174.58° and the N–Cu–O angles are 88.52–99.08°. One $[SiW_{12}O_{40}]^{4-}$ connects the other $[SiW_{12}O_{40}]^{4-}$ by Cu1 and O12 to form the 1-D chain structure. The distance of Cu ions in adjacent chains is about 9 Å.

3.3. *FTIR spectroscopy and thermogravimetric analysis*

IR spectra exhibit characteristic peaks for the α-Keggin structure at 947, 898, and 785 cm^{-1} for **1** (Supplementary material). The signals at 956, 906, and 786 cm^{-1} can be attributed to ν_{as}(W–Od), ν_{as}(Si–O), and ν_{as}(W–Oc–W) bands, respectively. Peaks at 1800–1100 cm^{-1} are characteristic of pyridine.

   The thermal gravimetric curve of **1** is shown in "Supplementary material." It shows a total weight loss of 18.34% from 50°C to 600°C. Weight loss of 12.55% at 50–310°C corresponds to loss of all non-coordinated and coordinated water molecules (Calcd 12%). The weight loss of 5.79% at 360–410°C arises from decomposition of organic molecules (Calcd 18.33%). The bond valence sum calculations [22] indicate that all tungsten atoms are in the highest oxidation state (+6), while all coppers are in the +1 oxidation state.

3.4. *Photoluminescence properties*

The luminescent properties of **1** in the solid state at room temperature upon excitation at 367 nm are depicted in figure 3. A broad intense emission at 460 nm can be found. In order to understand the nature of such emission, the luminescence of free pyridine is also measured, which shows an emission at 465 nm upon excitation at 280 nm (Supplementary material). The emission peaks at 460 nm for **1** may be assigned to metal-to-ligand charge transfer [23]. According to emission spectra of other Cu(I)-compounds, the 460 nm peak observed in **1** should be attributed to pyridine emission, which means that energy transfer to Cu(I)-based states competes with emission from

Cu(I) ion [24]. Based on the emission spectra of **1**, there is 5 nm blue-shift from the emission of pyridine, and increased emission intensity in comparison with the emission intensity of pyridine. There is about 5 nm blue-shift from the emission of pyridine in the emission spectra of **1**, and a stronger emission intensity than emission spectra of pyridine.

3.5. *Catalysis active*

The catalytic activity of **1** has been assessed in catalyzing the Ullmann diaryl ether synthesis [25]. Benzene chloride (2 mmol), phenol (2.5 mmol), K_3PO_4 (425 mg, 2.0 mmol), **1** (1 mol %), and DMF (0.5 mL) are mixed. The system is stirred at 100°C under an argon environment for 48 h, cooled to room temperature and then diluted with dichloromethane (15 mL). The mixture is filtered and sediment washed with 15 mL dichloromethane. (^{1}H NMR (ppm): δ 7.32–7.36, 7.10, 7.01. ^{13}C NMR (ppm): δ 157.1, 128.9, 123.3, 118.5. MS m/z 170(M+), 140, 77, 66, 51, 38. Anal. Calcd for $C_{12}H_{10}O$: C, 84.67; H, 5.91. Found: C, 84.57; H, 5.90). The catalytic activity of **1** is higher than CuBr catalyst under the same conditions.
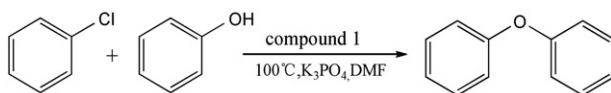
4. Conclusions

A POMs-based Cu(I) organic–inorganic hybrid compound $\{[Cu(py)_2]_4[SiW_{12}O_{40}]\}$ has been synthesized from hydrothermal decarboxylation. The Cu(II) is reduced to Cu(I) by the reductant triethylamine. The luminescence of **1** indicates that the emission can be assigned to Cu(I) to pyridine charge transfer. The 1-D chain complex efficiently catalyzes the *O*-arylation of both phenols and aryl halides because of the presence of active and air-stable Cu(I). Significantly, introducing of reductant and decarboxylation reaction is crucial for the synthesis of **1**, which provides a new route for synthesis of organic–inorganic hybrid compounds.

Supplementary material

CCDC-843099 for **1** contains supplementary crystallographic data for this article. This data can be obtained free of charge at www.ccdc.cam.ac.uk/conts/retrieving.html (or from the Cambridge Crystallographic Data Centre, 12 Union Road, Cambridge CB2 1EZ, UK; Fax: t44-1223/336-033; Email: deposit@ccdc.cam.ac.uk).

Acknowledgments

References

[1] M.T. Pope. *Heteropoly and Isopoly Oxometalates*, Springer-Verlag, Berlin (1983).
[2] M.T. Pope, A. Müller. *Angew. Chem., Int. Ed. Engl.*, **30**, 34 (1991).
[3] C. Zhang, P.T. Ma, H.N. Chen, J.P. Wang, J.Y. Niu. *J. Coord. Chem.*, **64**, 2178 (2011).
[4] L.J. Chen, D.Y. Shi, Y. Wang, H.L. Cheng, Z.D. Geng, J.W. Zhao, P.T. Ma, J.Y. Niu. *J. Coord. Chem.*, **64**, 400 (2011).
[5] J. Miao, S.X. Zhang, S.J. Li, Y.H. Gao, X. Zhang, X.N. Wang, S.X. Liu. *J. Coord. Chem.*, **64**, 4006 (2011).
[6] S. Alvarez. *Coord. Chem. Rev.*, **193**–**195**, 13 (1999).
[7] B.J. Hathaway. In *Comprehensive Coordination Chemistry*, G. Wilkinson, R.D. Gillard, J.A. McCleverty (Eds), Vol. 5, Pergamon Press, Oxford (1987).
[8] S. Jagner, G. Helgesson. *Adv. Inorg. Chem.*, **37**, 1 (1991).
[9] P.G. Eller, D.C. Bradley, M.B. Hursthouse, D.W. Meek. *Coord. Chem. Rev.*, **24**, 1 (1977).
[10] E. Solomon, R. Sarangi, J. Woertink, A. Augustine, J. Yoon, S. Ghosh. *Acc. Chem. Res.*, **40**, 581 (2007).
[11] T. Punniyamurthy, L. Rout. *Coord. Chem. Rev.*, **252**, 134 (2008).
[12] L.M. Mirica, X. Ottenwaelder, T.D.P. Stack. *Chem. Rev.*, **104**, 1013 (2004).
[13] N.F.M. Henry, K. Lonsdale (Eds). *International Tables for X-ray Crystallography*, Kynoch Press, Birmingham (1952).
[14] G.M. Sheldrick. *SHELX-97, Program for Crystal Structure Solution*, University of Göttingen, Göttingen, Germany (1997).
[15] C.D. Wu, C.Z. Lu, H.H. Zhuang, J.S. Huang. *Inorg. Chem.*, **41**, 5636 (2002).
[16] L.L. Chen, L. Zhang, Y.R. Gao, L.Y. Pang, G.L. Xue, F. Fu, J.W. Wang. *J. Coord. Chem.*, **62**, 2832 (2008).
[17] J.P. Wang, Y.Q. Feng, P.T. Ma, J.Y. Niu. *J. Coord. Chem.*, **62**, 1895 (2009).
[18] L. Yin, M. Kanai, M. Shibasaki. *J. Am. Chem. Soc.*, **131**, 9619 (2009).
[19] S.J. Hong, S.M. Huber, L. Gagliardi, C.C. Cramer, W.B. Tolman. *J. Am. Chem. Soc.*, **129**, 14190 (2007).
[20] H.J. Pang, C.J. Zhang, Y.G. Chen, D.M. Shi. *J. Coord. Chem.*, **63**, 418 (2010).
[21] F. Yao, F.X. Meng, Y.G. Chen, C.J. Zhang. *J. Coord. Chem.*, **63**, 196 (2010).
[22] I.D. Brown, D. Altermatt. *Acta Crystallogr. Sect. B: Struct. Sci.*, **41**, 244 (1985).
[23] W. Chen, J.-Y. Wang, J. Chen, Q. Yue, H.-M. Yuan, J.-S. Chen, S.-N. Wang. *Inorg. Chem.*, **42**, 944 (2003).
[24] M.D. Allendorf, C.A. Bauer, R.K. Bhakta, R.J.T. Houk. *Chem. Soc. Rev.*, **38**, 1330 (2009).
[25] F. Ullmann. *Ber. Dtsch. Chem. Ges.*, **37**, 853 (1904).